

## Shape oscillations of a viscoelastic droplet suspended in a viscoelastic host liquid

Fang Li,\* Xie-Yuan Yin, and Xie-Zhen Yin

*Department of Modern Mechanics, University of Science and Technology of China, Hefei, Anhui 230027, People's Republic of China*



(Received 29 November 2019; accepted 2 March 2020; published 19 March 2020)

A study on the small-amplitude oscillation of a viscoelastic droplet suspended in an immiscible viscoelastic host liquid is carried out. The viscoelasticity of the inner and outer liquids is described by Jeffreys constitutive equation. The analytical characteristic equation is derived and the complex frequency is solved numerically. The effect of the outer host liquid on the oscillation of the droplet is examined for the fundamental mode  $n = 2$ . It is found that the damping rate and the frequency of oscillation of the droplet are decreased as the host liquid gets denser in the inviscid case. The boundaries between periodic oscillation and aperiodic decay in the parametric plane of the Ohnesorge number and the relative stress relaxation time are captured. The viscosity of the outer liquid makes the supercritical and subcritical bifurcation phenomena disappear and leads to periodic oscillations of the droplet all the time. Moreover, the viscosity of the outer liquid exhibits a dual effect on the decay of the amplitude of oscillation. The elasticity of the outer liquid affects the oscillation of the droplet monotonically: the stress relaxation time decreases the damping rate and the frequency of oscillation of the droplet, whereas the strain retardation time increases them limitedly.

DOI: [10.1103/PhysRevFluids.5.033610](https://doi.org/10.1103/PhysRevFluids.5.033610)

### I. INTRODUCTION

Shape oscillations of liquid droplets occur in diverse applications, including emulsion, extraction, spraying, ink-jet printing, interfacial and rheological property measurement, mass and heat transfer, biological systems, and so on. Since the pioneer work of Rayleigh [1], Kelvin [2], and Lamb [3], linear oscillations of Newtonian viscous/inviscid droplets have been extensively studied by many researchers, e.g., Chandrasekhar [4], Reid [5], Prosperetti [6], Arcidiacono *et al.* [7], among others. More recently, the rheological properties of liquid have been taken into account in the study of small-amplitude oscillations of droplets. It has been found that bulk viscoelasticity may influence the oscillation behavior of a droplet significantly. Bauer [8] and Bauer and Eidel [9] explored the surface and interface vibrational behavior of spherical viscoelastic systems. Khismatullin and Nadim [10] revealed that there exists a type of shape oscillation induced by elasticity, which does not depend on surface tension. Brenn and Teichtmeister [11] proposed a proof-of-concept experiment to determine the deformation retardation time of a viscoelastic liquid through linear shape oscillations of the droplet. The method was later tested by Brenn and Pohl [12]. Hoath *et al.* [13] carried out an experimental study on the oscillation behavior of a non-Newtonian liquid droplet in drop-on-demand ink-jet printing.

Beyond the linear scope, large-amplitude oscillations of droplets are of practical importance. The experimental investigation showed that when the amplitude of oscillation exceeds 10% of

---

\*fli6@ustc.edu.cn

the drop radius the nonlinear effect cannot be neglected [14]. In addition to the axisymmetric quadrupole mode  $n = 2$ , large-amplitude oscillations of the multilobed and polyhedral modes were also observed in experiments [15]. Trinh *et al.* [16] found in the experiment the resonant coupling between higher- and lower-order modes. The nonlinear oscillation behavior of viscous droplets was numerically studied by Basaran [17], Shi and Apfel [18], Rush and Nadim [19], etc. Smith [20] derived the modulation equations for nonlinear oscillations of a viscous drop and found that the liquid in the drop may undergo abrupt changes in comparison to the small-amplitude case if the amplitude of oscillation exceeds 20% of the drop radius.

Two-fluid systems have also been considered by some researchers. Miller and Scriven [21] derived for the first time a general characteristic equation describing small-amplitude oscillations of a viscous droplet immersed in an immiscible viscous host liquid. Prosperetti [22] calculated numerically the damping rate and the angular frequency of oscillation of a viscous drop in an immiscible viscous liquid. Marston [23] investigated the forced shape deformation of a two-fluid spherical system in the presence of the interface stresses produced by superimposed acoustic waves. Basaran *et al.* [24] carried out a relevant experimental investigation and found that linear theory agrees well with the experimental results as long as the drop radius is smaller than a critical value. Bayazitoglu and Suryanarayana [25] solved the oscillation frequency and the damping rate for a liquid-liquid system using a more accurate numerical method and compared the theoretical predictions with the existing experimental data. Whitaker *et al.* [26] took into account evaporation in the small-amplitude shape oscillation of a superfluid helium drop surrounded by saturated helium vapor. Chrispell *et al.* [27] developed a two-dimensional Navier-Stokes immersed boundary algorithm to simulate the dynamics of a viscoelastic droplet suspended in a viscoelastic matrix. There are also a number of studies of Newtonian/non-Newtonian drops suspended in a shear, extensional or rotating flow of Newtonian/non-Newtonian liquid. Interested readers are referred to, among others, the references [28–33].

In the present paper, we extend the work of the former researchers [10,11,21,22] to the case of a non-Newtonian viscoelastic liquid droplet immersed in an immiscible viscoelastic host liquid. A general characteristic equation is derived for the complex frequency. The damping rate and the angular frequency describing the shape oscillation of the viscoelastic droplet are solved numerically. The effect of the density, viscosity and elasticity of the outer host liquid on the oscillation behavior of the viscoelastic droplet is highlighted. In Sec. II the theoretical model is formulated; in Sec. III the numerical results are presented and discussed; in Sec. IV the main conclusion is drawn.

## II. THEORETICAL MODEL

An isolate spherical liquid droplet is stationarily suspended in an unbounded host liquid. Naturally, the spherical coordinate system  $(r, \theta, \varphi)$  with the origin located at the center of the droplet is adopted to describe the problem, where  $r$ ,  $\theta$ , and  $\varphi$  are the radius, the polar angle, and the azimuthal angle, respectively. The droplet and the outer host liquid are immiscible. The effect of the gravity and buoyancy forces is considered to be negligible. There is no relative motion between the droplet and the host liquid. Before the system is perturbed, the pressure difference at the liquid-liquid interface is balanced by the interfacial tension, i.e.,  $P_i - P_o = 2\gamma/R$ , where  $P$  is the basic pressure,  $\gamma$  is the interfacial tension coefficient, and  $R$  is the radius of the droplet. Hereafter, the subscripts  $i$  and  $o$  are used to denote the quantities pertaining to the inner droplet and the outer host liquid, respectively.

Both the inner and outer liquids are assumed to be non-Newtonian viscoelastic. Their viscoelasticity is modeled by the linear Jeffreys constitutive equation,

$$\boldsymbol{\tau} + \lambda_1 \frac{\partial \boldsymbol{\tau}}{\partial t} = 2\eta_0 \left( \mathbf{D} + \lambda_2 \frac{\partial \mathbf{D}}{\partial t} \right), \quad (1)$$

where  $\boldsymbol{\tau}$  is the deviatoric stress tensor,  $t$  is the time,  $\mathbf{D} (= \frac{1}{2}[\nabla \mathbf{v} + (\nabla \mathbf{v})^T])$  with  $\mathbf{v}$  the velocity and the superscript  $T$  denoting the transpose) is the rate-of-strain tensor,  $\eta_0$  is the zero-shear viscosity,

$\lambda_1$  is the stress relaxation time, and  $\lambda_2$  is the strain retardation time. For brevity, the subscripts  $i$  and  $o$  are dropped in the equations applicable to both liquids.

After being disturbed by an infinitesimal perturbation, the system is governed by the following linearized equations:

$$\nabla \cdot \mathbf{v} = 0, \quad (2)$$

$$\rho \frac{\partial \mathbf{v}}{\partial t} = -\nabla p + \nabla \cdot \boldsymbol{\tau}, \quad (3)$$

where  $\rho$  is the density and  $p$  is the pressure perturbation.

At the deformed liquid-liquid interface  $r = R + \xi$ , where  $\xi$  is the displacement of the interface deviating from its equilibrium position, the linearized kinematic boundary condition requires that

$$v_r = \frac{\partial \xi}{\partial t}, \quad (4)$$

where  $v_r$  is the velocity component in the radial direction, the no-slip condition requires that

$$v_{\theta,i} = v_{\theta,o}, \quad v_{\varphi,i} = v_{\varphi,o}, \quad (5)$$

where  $v_\theta$  and  $v_\varphi$  are, respectively, the velocity components in the polar and azimuthal directions, the balance of the tangential stresses is formulated as

$$\tau_{r\theta,i} = \tau_{r\theta,o}, \quad \tau_{r\varphi,i} = \tau_{r\varphi,o}, \quad (6)$$

where  $\tau_{r\theta}$  and  $\tau_{r\varphi}$  are, respectively, the  $r\theta$ - and  $r\varphi$ -components of the stress tensor  $\boldsymbol{\tau}$ , and the balance of the forces in the normal direction is

$$-p_o + \tau_{rr,o} + p_i - \tau_{rr,i} = \gamma \nabla \cdot \mathbf{n}, \quad (7)$$

where  $\tau_{rr}$  is the  $rr$ -component of  $\boldsymbol{\tau}$ ,  $\mathbf{n}$  is the outward unit normal vector, and  $\nabla \cdot \mathbf{n}$  is twice the surface curvature.

In linear analysis, the perturbation is supposed to be of normal mode form, that is,

$$(\xi, \mathbf{v}, p, \boldsymbol{\tau}) = [\hat{\xi}, \hat{\mathbf{v}}(r), \hat{p}(r), \hat{\boldsymbol{\tau}}(r)] P_n^m(\cos\theta) e^{im\varphi} e^{-\sigma t}, \quad (8)$$

where the hat denotes the initial amplitude of the perturbation,  $P_n^m(\cos\theta)$  is the associated Legendre polynomial with the indices  $n$  and  $m$  (integers,  $0 \leq m \leq n$ , and  $n \leq 2$ ), the superscript  $i$  is the imaginary unit, and  $\sigma$  is the complex frequency whose real part and imaginary part are the so-called damping rate and the angular frequency of oscillation, respectively.

Substituting the normal mode decomposition Eq. (8) into the constitutive Eq. (1), the governing Eqs. (2) and (3), and the boundary condition Eqs. (4)–(7), a characteristic equation can be derived for the complex frequency  $\sigma$ . The details of the derivation process can be found in the Appendix.

Choosing the density  $\rho_i$ , the zero-shear viscosity  $\eta_{0,i}$ , the radius  $R$ , the capillary time  $t_{c,i} = \sqrt{\rho_i R^3 / \gamma}$ , and the capillary force  $\gamma/R$  as the scales, the characteristic equation is nondimensionalized as

$$\frac{\omega_0^2}{\omega^2} = \frac{[(2n+1)P_{n+\frac{1}{2}}(z_i) + 2n(n+2)(\eta_{0r} \frac{\zeta_o}{\zeta_i} - 1)][(2n+1)\eta_{0r} \frac{\zeta_o}{\zeta_i} Q_{n+\frac{1}{2}}(z_o) - 2(n-1)(n+1)(\eta_{0r} \frac{\zeta_o}{\zeta_i} - 1)]}{z_i^2 (n\rho_r + n+1) [P_{n+\frac{1}{2}}(z_i) + \eta_{0r} \frac{\zeta_o}{\zeta_i} Q_{n+\frac{1}{2}}(z_o) + 2(\eta_{0r} \frac{\zeta_o}{\zeta_i} - 1)]} - 1, \quad (9)$$

where  $\omega$  is the nondimensional counterpart of the complex frequency  $\sigma$ ,  $\omega_0$  is the nondimensional complex frequency of the inviscid problem,

$$\omega_0^2 = \frac{(n-1)n(n+1)(n+2)}{n\rho_r + n+1}, \quad (10)$$

$$\zeta_i = \frac{1 - \lambda_{2r,i}\omega}{1 - \lambda_{1r,i}\omega}, \quad \zeta_o = \frac{1 - \lambda_{2r,o}\omega}{1 - \lambda_{1r,o}\omega}, \quad (11)$$

$$z_i = \sqrt{\frac{\omega}{\text{Oh}\zeta_i}}, \quad z_o = \sqrt{\frac{\rho_r\omega}{\eta_{0r}\text{Oh}\zeta_o}}, \quad (12)$$

$$P_{n+\frac{1}{2}}(z_i) = z_i \frac{J_{n+\frac{1}{2}}(z_i)}{J_{n+\frac{3}{2}}(z_i)}, \quad Q_{n+\frac{1}{2}}(z_o) = z_o \frac{H_{n+\frac{1}{2}}^{(1)}(z_o)}{H_{n-\frac{1}{2}}^{(1)}(z_o)}, \quad (13)$$

$J_{n+\frac{1}{2}}$  and  $H_{n+\frac{1}{2}}^{(1)}$  are the Bessel and Hankel functions of the first kind, respectively.

The dimensionless parameters appearing in the characteristic Eq. (9) are: the density ratio of the outer to inner liquid  $\rho_r = \rho_o/\rho_i$ , the viscosity ratio of the outer to inner liquid  $\eta_{0r} = \eta_{0,o}/\eta_{0,i}$ , the Ohnesorge number of the inner liquid  $\text{Oh} = \eta_{0,i}/\sqrt{\rho_i\gamma R}$ , the relative stress relaxation time of the inner liquid  $\lambda_{1r,i} = \lambda_{1,i}/t_{c,i}$ , the relative strain retardation time of the inner liquid  $\lambda_{2r,i} = \lambda_{2,i}/t_{c,i}$ , the relative stress relaxation time of the outer liquid  $\lambda_{1r,o} = \lambda_{1,o}/t_{c,i}$ , and the relative strain retardation time of the outer liquid  $\lambda_{2r,o} = \lambda_{2,o}/t_{c,i}$ .

Some limit cases can be obtained from Eq. (9):

(1) A viscoelastic liquid droplet suspended in a vacuum.

Let the dimensionless parameters  $\rho_r$ ,  $\eta_{0r}$ ,  $\lambda_{1r,o}$ , and  $\lambda_{2r,o}$  be zero, and the characteristic Eq. (9) reduces to that for a viscoelastic liquid droplet suspended in a vacuum, i.e.,

$$\frac{\omega_0^2}{\omega^2} = \frac{2(n-1)[(2n+1)P_{n+\frac{1}{2}}(z_i) - 2n(n+2)]}{z_i^2(P_{n+\frac{1}{2}}(z_i) - 2)} - 1, \quad (14)$$

where  $\omega_0^2 = (n-1)n(n+2)$  with  $\omega_0$  the dimensionless complex frequency in the inviscid case. Equation (14) is the same with the characteristic equations presented by Khismatullin and Nadim [10] and Brenn and Teichtmeister [11].

(2) A gas bubble suspended in a viscoelastic host liquid.

Assume that the hydrodynamic effect of the gas is negligible. In the dimensional characteristic Eq. (A34), if we set all the parameters of the inner liquid to zero, we can get a characteristic equation describing the oscillation of a gas bubble in a viscoelastic liquid, which is expressed in nondimensional form as

$$\frac{\omega_0^2}{\omega^2} = \frac{2(n+2)[(2n+1)Q_{n+\frac{1}{2}}(z_o) - 2(n-1)(n+1)]}{z_o^2(Q_{n+\frac{1}{2}}(z_o) + 2)} - 1, \quad (15)$$

where  $\omega_0^2 = (n-1)(n+1)(n+2)$  with  $\omega_0$  the complex frequency in the corresponding inviscid case, and  $z_o = \sqrt{\omega/\text{Oh}\zeta_o}$ . The other symbols are the same as defined previously. Note that in the bubble case the capillary time of the outer liquid,  $t_{c,o} = \sqrt{\rho_o R^3/\gamma}$ , is used as the time scale instead. As a consequence, the definition of the relevant dimensionless parameters are  $\text{Oh} = \eta_{0,o}/\sqrt{\rho_o\gamma R}$ ,  $\lambda_{1r,o} = \lambda_{1,o}/t_{c,o}$ , and  $\lambda_{2r,o} = \lambda_{2,o}/t_{c,o}$ . It is proved that Eq. (15) is in accordance in form with the characteristic equation derived by Miller and Scriven [21] for a gas bubble in a viscous liquid.

(3) A viscous droplet suspended in a viscous host liquid.

If all the dimensionless parameters related to elasticity, i.e.,  $\lambda_{1r,i}$ ,  $\lambda_{2r,i}$ ,  $\lambda_{1r,o}$ , and  $\lambda_{2r,o}$ , are taken to be zero, then the characteristic Eq. (9) will be reduced to the one for small-amplitude oscillations of a purely viscous droplet in a purely viscous liquid. For the viscous case, different forms of characteristic equation were presented by Miller and Scriven [21], Prosperetti [22], and Basaran *et al.* [24], although they are in effect the same. In comparison, Prosperetti's expression is more simplified. Our derivation follows the work of Prosperetti [22].

### III. NUMERICAL RESULTS

The dimensionless complex frequency  $\omega$  is obtained by solving numerically the transcendental Eq. (9) using the Muller method in IMSL [34]. The code was checked by comparing with the results in Refs. [11,22]. It should be stressed that Eq. (9) has infinite discrete roots due to liquid viscosity.

The root having the smallest real part determines the oscillation characteristics of the droplet. Hence, we focus on this root most of time and just call it the least damped mode. Moreover, we consider only the quadrupole mode  $n = 2$ , since it is usually less damped than those higher-order modes. Note that the azimuthal wavenumber  $m$  does not appear in Eq. (9), which can be simply set to zero at the beginning [10,11]. The strain retardation time is basically one order of magnitude smaller than the stress relaxation time [11]. Without loss of generality, we take  $\lambda_{2r} = \lambda_{1r}/10$  in the calculation, unless specified otherwise.

### A. Effect of the density of the outer liquid on the oscillation of the viscoelastic droplet

The effect of the density of the outer liquid is studied by assuming that the outer host liquid is a Newtonian inviscid liquid. Thus the characteristic Eq. (9) reduces to

$$\frac{\omega_0^2}{\omega^2} = \frac{2(n-1)(n+1)[(2n+1)P_{n+\frac{1}{2}}(z_i) - 2n(n+2)]}{z_i^2(n\rho_r + n+1)[P_{n+\frac{1}{2}}(z_i) - 2]} - 1. \quad (16)$$

Only one dimensionless parameter related to the outer liquid, i.e., the density ratio  $\rho_r$ , appears in Eq. (16).

Figure 1 shows the variation of the damping rate  $\text{Re}(\omega)$  and the angular frequency  $\text{Im}(\omega)$  with the Ohnesorge number of the inner liquid  $\text{Oh}$  for different values of the density ratio  $\rho_r$ , where the elasticity of the inner liquid is assumed to be large. In the absence of the outer host liquid ( $\rho_r = 0$ ), the damping rate  $\text{Re}(\omega)$  grows almost linearly with the Ohnesorge number  $\text{Oh}$  from zero, as shown in Fig. 1(a). When  $\text{Oh}$  exceeds a critical value  $\text{Oh}_{\text{cr}}$ , a supercritical bifurcation takes place and the curve is divided into two branches, which are in effect two different modes. The damping rate of the upper branch increases rapidly with  $\text{Oh}$ , whereas the lower branch decreases gradually and behaves asymptotically as  $\text{Oh}$  goes to infinity. When  $\text{Oh} < \text{Oh}_{\text{cr}}$ , the droplet undergoes periodic oscillations, since it possesses nonzero angular frequency  $\text{Im}(\omega)$ , as shown in Fig. 1(b). When  $\text{Oh} > \text{Oh}_{\text{cr}}$ , the angular frequency is zero, implying that the droplet is overdamped and returns to its original spherical shape aperiodically. Apparently the critical Ohnesorge number  $\text{Oh}_{\text{cr}}$  gives not only the maximum damping rate but also the transition point from periodic to aperiodic decay of the least damped mode. In the case of periodic oscillation, viscosity induces energy dissipation and accelerates the damping of the perturbation. However, in the case of aperiodic decay, viscosity slows down the damping of the perturbation, resulting from vorticity diffusion in the liquid bulk that decreases velocity gradients and attenuates viscous dissipation of energy.

The density of the outer host liquid affects the behavior of the droplet greatly. As shown in Fig. 1, with  $\rho_r$  increasing, the critical Ohnesorge number  $\text{Oh}_{\text{cr}}$  gets larger, and the interval of  $\text{Oh}$  within which periodic oscillations take place is widened. It is possibly because that the existence of the outer inviscid liquid reduces the level of energy dissipation of the system and hence makes the transition from periodic to aperiodic decay occur at a larger viscosity of the inner liquid. For the same reason, the damping rate in the periodic oscillation case is decreased with  $\rho_r$  increasing. In Fig. 1(b), at  $\text{Oh} = 0$ , the oscillation frequency  $\text{Im}(\omega)$  decreases as  $\rho_r$  increases, a fact that can be seen directly from Eq. (10). As a consequence, at small values of  $\text{Oh}$ , the denser the outer liquid, the smaller the frequency of oscillation. But the trend is reversed at moderate  $\text{Oh}$ 's near  $\text{Oh}_{\text{cr}}$ . In the aperiodic decay case, the density ratio increases the damping rate of the least damped mode limitedly.

The effect of the outer inviscid liquid on the oscillation characteristics of the droplet at a small elasticity of the inner liquid is shown in Fig. 2. Compared with the large elasticity case shown in Fig. 1, the critical value of Ohnesorge number  $\text{Oh}_{\text{cr}}$  at which the supercritical bifurcation takes place is decreased to around 1 and the interval of Ohnesorge number for periodic oscillations is greatly narrowed down. Moreover, a subcritical bifurcation appears at a relatively large critical value of Ohnesorge number denoted by  $\text{Oh}'_{\text{cr}}$ . The lower branch of the subcritical bifurcation is exactly the upper branch of the supercritical bifurcation, as shown in Fig. 2(a). The damping rate of the upper branch of the subcritical bifurcation is large and is decreased as  $\text{Oh}$  increases. Beyond  $\text{Oh}'_{\text{cr}}$ , the

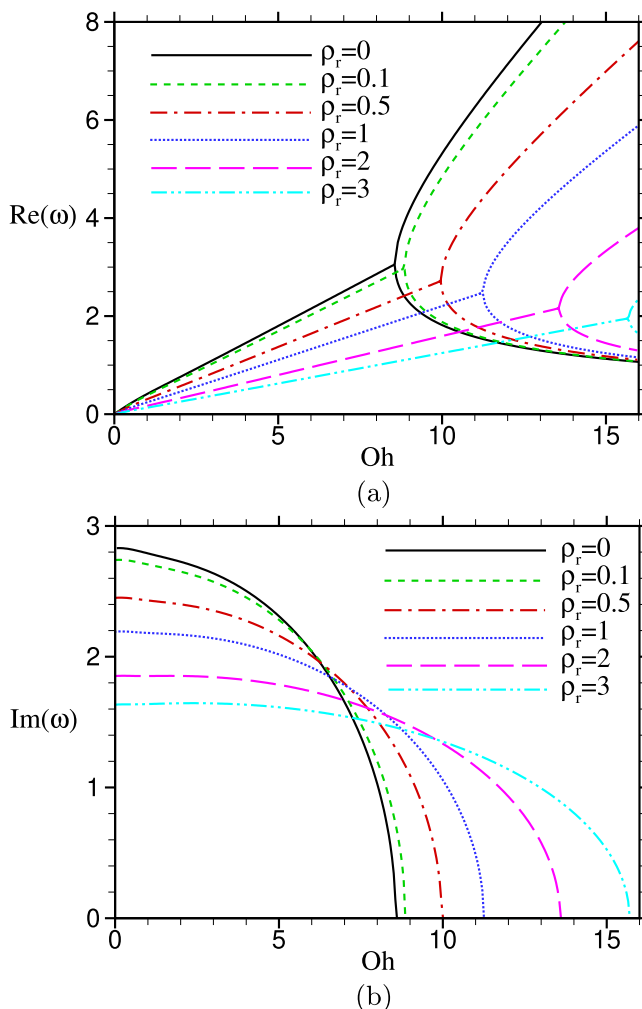


FIG. 1. (a) The damping rate  $Re(\omega)$  and (b) the angular frequency  $Im(\omega)$  versus the Ohnesorge number of the inner liquid  $Oh$  for different values of the density ratio  $\rho_r$ . The case of relatively large elasticity of the inner liquid,  $\lambda_{1r,i} = 30$ ,  $\lambda_{2r,i} = 3$ .

upper and lower branches coalesce and the damping rate ascends linearly with  $Oh$ ; meanwhile, the angular frequency is increased, see Fig. 2(b). As illustrated in the figure, increasing  $\rho_r$  impels both supercritical and subcritical bifurcation points, especially the latter, to move towards large Ohnesorge numbers. Within the periodic oscillation interval of  $Oh$  to the left of the supercritical bifurcation point, the influence of the outer liquid is analogous to that in the large elasticity case in Fig. 1. Within the oscillation interval to the right of the subcritical bifurcation point, both the damping rate and the angular frequency are decreased by the outer inviscid liquid.

For a viscoelastic liquid droplet, the case of large viscosity is of particular interest. As is well known, when viscosity is sufficiently large, a purely viscous liquid droplet is overdamped and experiences no periodic oscillation. However, if one adds some polymer into the liquid, then the droplet may oscillate again. It was deduced that this kind of oscillation is due to elasticity [10, 11]. The release of elastic potential energy overcomes viscous resistances and induces periodic oscillations of the droplet. However, elasticity cannot be infinitely large. If the stress relaxation time

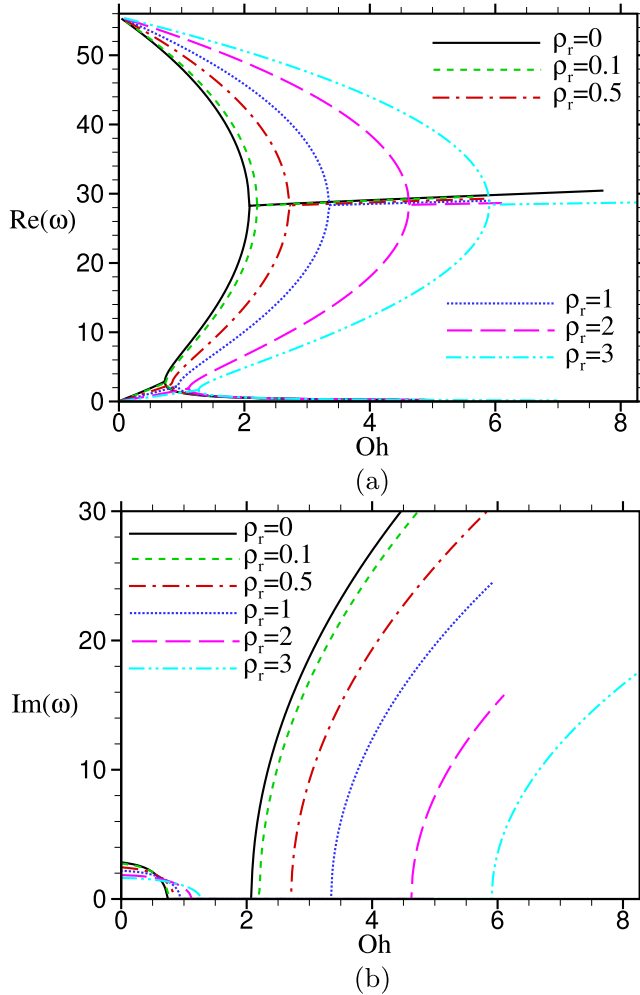


FIG. 2. (a) The damping rate  $Re(\omega)$  and (b) the angular frequency  $Im(\omega)$  versus the Ohnesorge number of the inner liquid  $Oh$  for different values of the density ratio  $\rho_r$ . The case of relatively small elasticity of the inner liquid,  $\lambda_{1r,i} = 0.018$ ,  $\lambda_{2r,i} = 0.0018$ .

is too large, then storing and releasing of elastic energy within every oscillation period gets hard, which does not favor periodic oscillations. Li *et al.* [35] highlighted the range of stress relaxation time for the occurrence of elasticity-induced periodic oscillation. Similar result is represented in Figs. 3(a) and 3(b), where the Ohnesorge number is fixed to 10. At such a large viscosity, the angular frequency for the corresponding purely viscous liquid ( $\lambda_{1r,i} = 0$ ) is zero, implying that the droplet undergoes no periodic oscillations. When the relative stress relaxation time  $\lambda_{1r,i}$  is located between 0.001 and 0.01, an abrupt increase in the angular frequency arises. Soon, the angular frequency reaches its maximum. As  $\lambda_{1r,i}$  increases further, the frequency is decreased. Ultimately, at a certain value of  $\lambda_{1r,i}$  (normally larger than 10), the angular frequency drops down to zero. For a periodically oscillatory droplet, elasticity diminishes its damping rate slightly. The transition from periodic oscillation to aperiodic decay at small elasticities is accomplished through a subcritical bifurcation, and the transition from periodic to aperiodic at large elasticities occurs at a supercritical bifurcation point. As the density ratio  $\rho_r$  increases, both the bifurcations, especially the supercritical one, are directed towards large values of  $\lambda_{1r,i}$ . The range of  $\lambda_{1r,i}$  for periodic oscillations

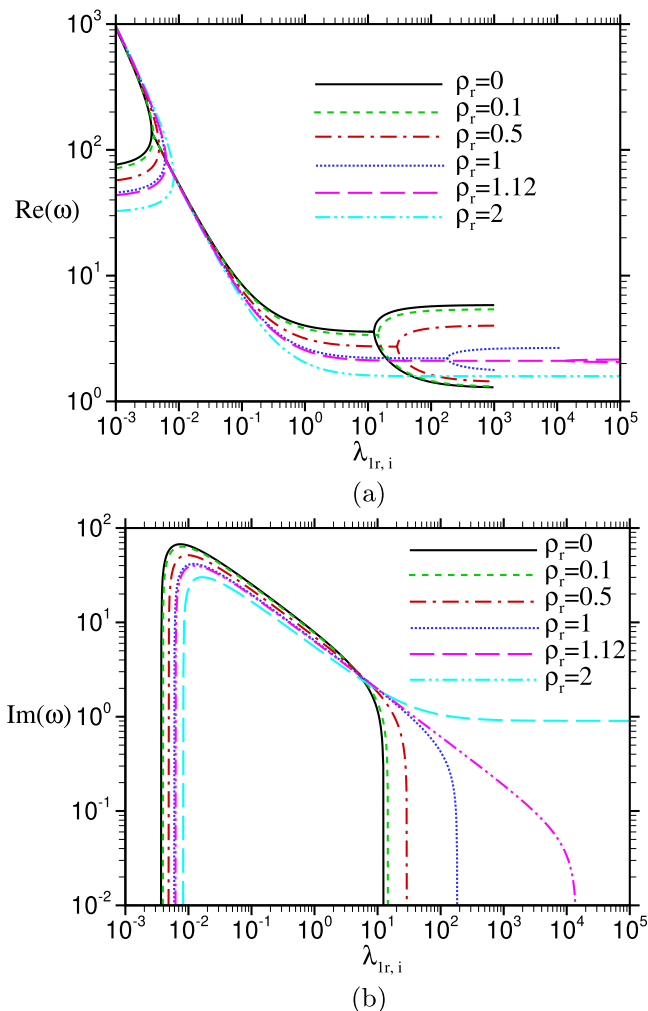


FIG. 3. (a) The damping rate  $\text{Re}(\omega)$  and (b) the angular frequency  $\text{Im}(\omega)$  versus the relative stress relaxation time of the inner liquid  $\lambda_{1r,i}$  for different values of the density ratio  $\rho_r$ . The case of relatively large viscosity of the inner liquid,  $\text{Oh} = 10$ .

is greatly broadened by increasing  $\rho_r$ . Particularly, when  $\rho_r$  becomes sufficiently large (see the line for  $\rho_r = 2$  in Fig. 3), the supercritical bifurcation phenomenon disappears, and the droplet maintains periodically oscillatory no matter how large the elasticity is. The mechanism in it may be that an inviscid host liquid can help fast storage and release of elastic energy at large elasticities.

The boundary between periodic oscillation and overdamped decay in the parametric plane of the relative stress relaxation time  $\lambda_{1r,i}$  and the Ohnesorge number  $\text{Oh}$  is illustrated in Fig. 4 for different values of the density ratio  $\rho_r$ . As shown in the figure, the left boundary consists of a straight oblique line (which is in practice a collection of subcritical bifurcation points like the one presented in Fig. 3) and an almost horizontal line (which is a collection of supercritical bifurcation points like the one shown in Fig. 2). The ends of the two lines form a sharp angle. The right boundary, which is practically a collection of supercritical bifurcation points like that illustrated in Fig. 1 or Fig. 3, is initially a straight oblique line, but bends slowly and becomes horizontal at large values of  $\lambda_{1r,i}$ . Between the left and right boundaries is the region in which the droplet undergoes periodic

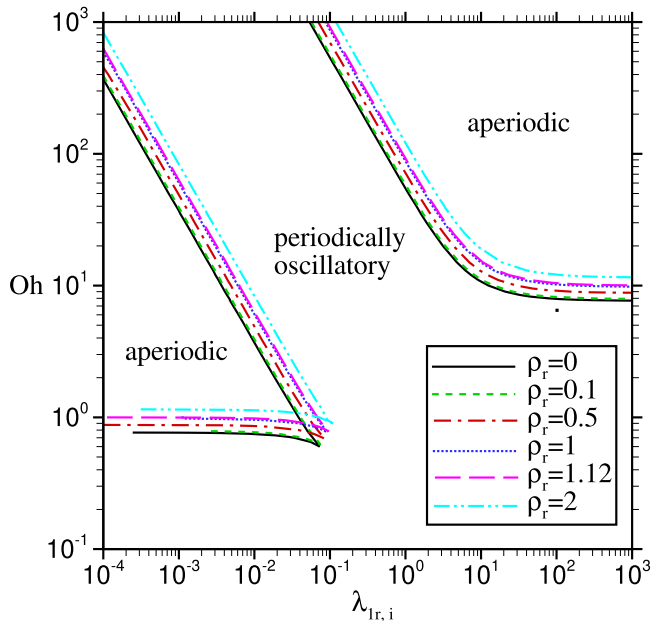


FIG. 4. The boundaries in the  $\lambda_{1r,i}$ -Oh plane.

oscillations with decreasing amplitude; in the other regions, the droplet experiences no oscillation and the perturbation is damped monotonically. Brenn and Teichtmeister [11] detected, in the plane of the Ohnesorge number  $Oh$  and the Deborah number  $De_1$  defined there, the boundary between surface tension-induced oscillation and aperiodic decay as well as the boundary between elasticity-induced oscillation and aperiodic decay, which are analogous in shape to the left boundary in Fig. 4. However, they did not examine large values of  $Oh$  and  $De_1$  and missed the right boundary between elasticity-induced oscillation and aperiodic decay as depicted in Fig. 4. It is of interest to note that the oblique straight lines of the left and right boundaries possess nearly the same slope (about  $-300$ ) in the log-log plot. It implies that as the viscosity of the inner liquid increases the range of  $\lambda_{1r,i}$  within which periodic oscillations occur is narrowed down. However, varying the density ratio  $\rho_r$  has no discernible influence on the slope. With the increase in  $\rho_r$ , the oblique lines move towards large values of  $\lambda_{1r,i}$ , and the Ohnesorge number at which the supercritical bifurcation vanishes is increased, in accordance with the trend illuminated in Fig. 3. The left horizontal boundary ascends as  $\rho_r$  increases, in accordance with the result illustrated in Fig. 2. Also note that when liquid viscosity is sufficiently small (the Ohnesorge number is smaller than a certain value, e.g., approximately 0.6 for  $\rho_r = 0$ ), as shown in Fig. 4, the droplet remains periodically oscillatory over the wide range of  $\lambda_{1r,i}$ . As  $\rho_r$  increases, this value of Ohnesorge number is increased to some extent.

The small viscosity case is shown in Fig. 5, where the Ohnesorge number of the inner liquid is taken to be 0.1. As shown in the figure, at such a small viscosity the droplet oscillates periodically over the whole range of  $\lambda_{1r,i}$ , in agreement with the result in Fig. 4. The effect of the density ratio  $\rho_r$  on the damping rate and the angular frequency is monotonic. As  $\rho_r$  increases, both are decreased visibly. That is, the existence of the outer inviscid liquid slows down the damping of the perturbation and prolongs the period of oscillation. As outlined previously, an inviscid host liquid lowers down the level of energy dissipation in a periodically oscillating system and in this way decreases the damping rate of the system. Moreover, the outer host liquid makes the liquid-liquid interface less free and diminishes the frequency of oscillation.

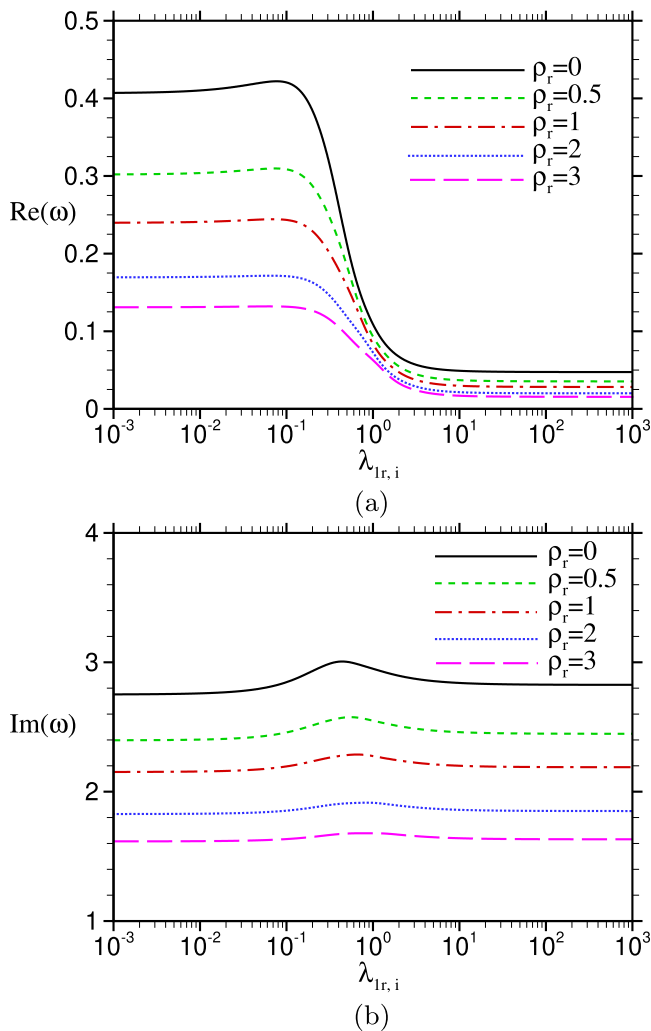


FIG. 5. (a) The damping rate  $\text{Re}(\omega)$  and (b) the angular frequency  $\text{Im}(\omega)$  versus the relative stress relaxation time of the inner liquid  $\lambda_{1r,i}$  for different values of the density ratio  $\rho_r$ . The case of relatively small viscosity of the inner liquid,  $\text{Oh} = 0.1$ .

### B. Effect of the viscosity of the outer liquid on the oscillation of the viscoelastic droplet

To study the effect of the viscosity of the outer liquid, we assume that the outer liquid is purely Newtonian viscous. The corresponding characteristic equation can be obtained by simply setting the parameter  $\zeta_o$  in Eq. (9) to 1. In such a case, there are two dimensionless parameters related to the outer liquid, i.e., the density ratio  $\rho_r$  and the viscosity ratio  $\eta_{0r}$ . As a matter of fact, the viscosity ratio  $\eta_{0r}$  is not an appropriate parameter representing the viscosity of the outer liquid, for in its definition the viscosity of the inner liquid  $\eta_{0,i}$  is used as the scale and varying  $\eta_{0,i}$  results in the change in  $\eta_{0r}$ . Here we introduce an alternative parameter, i.e., the Ohnesorge number of the outer liquid defined as  $C = \eta_{0,o}/\sqrt{\rho_o\gamma\bar{R}}$ , to reflect the relative importance of the viscosity of the outer liquid. The relationship of  $C$  and  $\eta_{0r}$  is  $C = \eta_{0r}\text{Oh}/\sqrt{\rho_r}$ .

Figure 6 shows the effect of the Ohnesorge number of the outer liquid  $C$  on the variation of the damping rate and the angular frequency with the Ohnesorge number of the inner liquid  $\text{Oh}$ , where

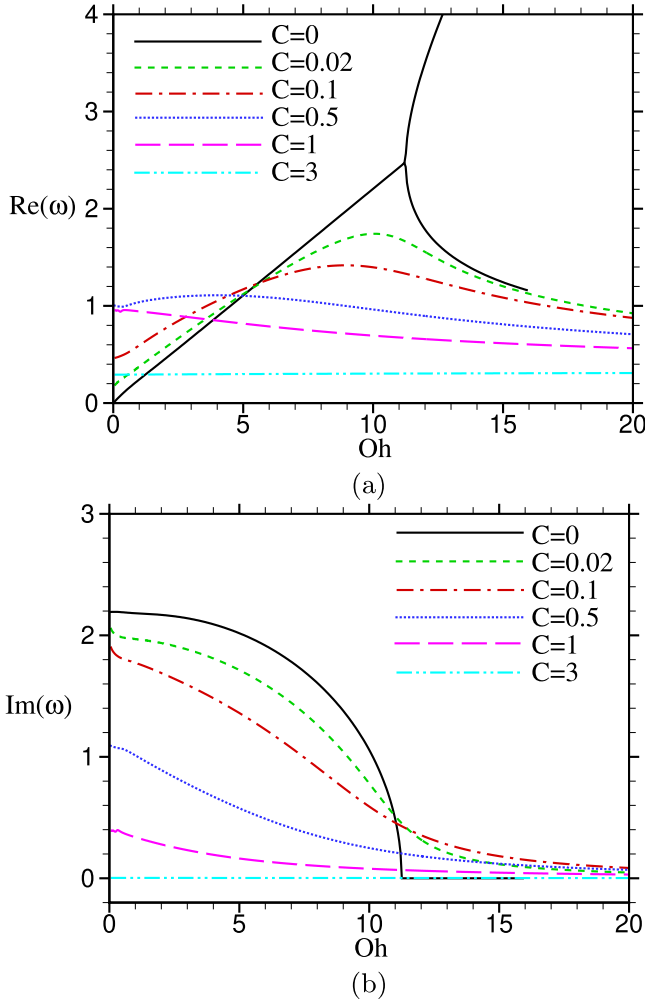


FIG. 6. (a) The damping rate  $Re(\omega)$  and (b) the angular frequency  $Im(\omega)$  versus the Ohnesorge number of the inner liquid  $Oh$  for different values of the Ohnesorge number of the outer liquid  $C$ . The case of relatively large elasticity of the inner liquid,  $\lambda_{1r,i} = 30$ ,  $\lambda_{2r,i} = 3$ ,  $\rho_r = 1$ .

the elasticity of the inner liquid is supposed to be large and the density ratio  $\rho_r$  is fixed to 1. It can be seen from the figure that the viscosity of the outer liquid affects greatly the oscillation characteristics of the droplet. Most intriguingly, when the outer liquid is viscous, the supercritical bifurcation phenomenon disappears. There are aperiodic branches no more. The droplet oscillates periodically over all values of  $Oh$ , only that its angular frequency  $Im(\omega)$  approaches zero asymptotically at large  $Oh$ 's. This behavior of the droplet is more similar to the case of a bubble in a viscous liquid than the case of a viscous droplet in a vacuum [22]. Probably the unboundedness of the host liquid and the concavity geometry of the free surface in the bubble case has a more profound effect than a confined liquid drop. From a mathematic point of view, the Hankel function in the characteristic Eq. (9) or Eq. (15) is always complex even when its argument is real. In such a case, the roots of the characteristic equations cannot be real, that is, the angular frequency is always nonzero, no matter how large the viscosity of the droplet or the outer liquid is. Physically, the infinite extent of the outer viscous liquid together with the no-slip boundary condition at the liquid-liquid interface smooths out large velocity gradients and diminishes viscous stresses in the bulk of the liquids.

As a result, energy dissipation due to viscosity is reduced and periodic oscillations takes place at larger viscosities. Differently, when its viscosity is small, the outer liquid indeed enhances energy dissipation and increases the damping rate. Generally, from the variation of the damping rate with  $Oh$  and  $C$  in Fig. 6(a), we see that the viscosity of the inner or outer liquid plays a dual role in the oscillation of the droplet: on one hand, viscosity dissipates energy and increases the damping rate; on the other hand, viscosity generates and diffuses vorticities, suppresses loss of energy, and tries to decrease the damping rate. Two mechanisms competes with each other: at small viscosities, the former prevails, whereas at large viscosities, the latter dominates. The balance between them is obtained at some critical value of  $Oh$  or  $C$ , at which the damping rate reaches its maximum. This critical  $Oh$  or  $C$  can be estimated by equaling the length of vorticity diffusion to the radius of the drop [6,22]. The angular frequency is decreased significantly by increasing  $C$  at relatively small values of  $Oh$ . At relatively large values of  $Oh$ , the angular frequency is first increased and then decreased with  $C$  increasing. When  $C$  is sufficiently large [see the line for  $C = 3$  in Fig. 6(b)], the angular frequency is nearly zero over the range of  $Oh$ , indicating that large viscosities do not benefit the periodic oscillation of the droplet.

The effect of the viscosity of the outer liquid on the damping rate and the angular frequency of the viscoelastic droplet when the elasticity of the inner liquid is small is shown in Fig. 7. Similar to the large elasticity case illustrated in Fig. 6, the bifurcations disappear when the outer liquid is viscous. The droplet is periodically oscillatory all the time. In Fig. 7(a), it appears that the upper and lower branches beyond the supercritical bifurcation point are separated and the lower branch joins the least damped mode. Similar to the large elasticity case, the viscosity of the inner or outer liquid exhibits a dual effect on the oscillation of the droplet. In Fig. 7(b), at small values of  $Oh$ , the angular frequency is greatly decreased by increasing the viscosity of the outer liquid. When  $C$  is increased to 2, the angular frequency is nearly zero for all  $Oh$ 's. At large values of  $Oh$ , the angular frequency is nonzero but quite small for all  $C$ 's.

The dependence of the damping rate and the angular frequency on the relative stress relaxation time of the inner liquid  $\lambda_{1r,i}$  is presented in Fig. 8 for different values of  $C$ , where the viscosity of the inner liquid is large. The inviscid case of the outer liquid ( $C = 0$ ) is also plotted in the figure for comparison. Clearly, when the outer liquid is viscous, the subcritical and supercritical bifurcations do not exist any more. The lower branch of the subcritical bifurcation and the upper branch of the supercritical bifurcation appear to become parts of an integrated mode. Meanwhile, the upper branch of the subcritical bifurcation and the lower branch of the supercritical bifurcation are integrated into a second mode, as depicted in Fig. 8(a). For a fixed value of  $C$ , the lines of the two modes intersect at some point. That is, the least damped mode shifts from one to the other. As illustrated in Fig. 8(b), both the modes are periodically oscillatory with nonzero angular frequency for all values of  $\lambda_{1r,i}$ . With an unbounded domain, the viscous host liquid removes the possibility of aperiodic decay of the perturbation. At small values of  $\lambda_{1r,i}$  close to zero, the viscosity of the outer liquid increases the damping rate and the angular frequency of the least damped mode slightly, whereas at large values of  $\lambda_{1r,i}$ , both the damping rate and the angular frequency of the mode are generally decreased by increasing  $C$ . These trends confirm the dual role the viscosity of the outer liquid plays in the oscillation behavior of the droplet.

The case of small viscosity of the inner liquid is also examined. The corresponding result is illustrated in Fig. 9, where the line for the inviscid case  $C = 0$  is plotted for comparison. In the figure, as  $C$  increases from zero to 0.03, the damping rate is increased, whereas the angular frequency is decreased. When  $C$  is further increased to 0.1, starting from  $\lambda_{1r,i} \simeq 0.1$ , the angular frequency is decreased rapidly as  $\lambda_{1r,i}$  increases. When  $\lambda_{1r,i}$  is around 80, the angular frequency almost falls to zero. In the figure, in addition to the least damped mode, the second least damped mode that possesses the second smallest damping rate is plotted for  $C = 0.1$ . (Note that around  $C = 0.1$  the viscosity of the outer liquid is comparable to the viscosity of the inner liquid.) It is demonstrated in Fig. 9(a) that the curves of the two modes encounter each other at  $\lambda_{1r,i} \simeq 80$  and form an analogy to supercritical bifurcation. Beyond the bifurcation point they seem to become two aperiodic branches. This scenario remains when  $C$  is increased to 0.2. However, when  $C$  becomes

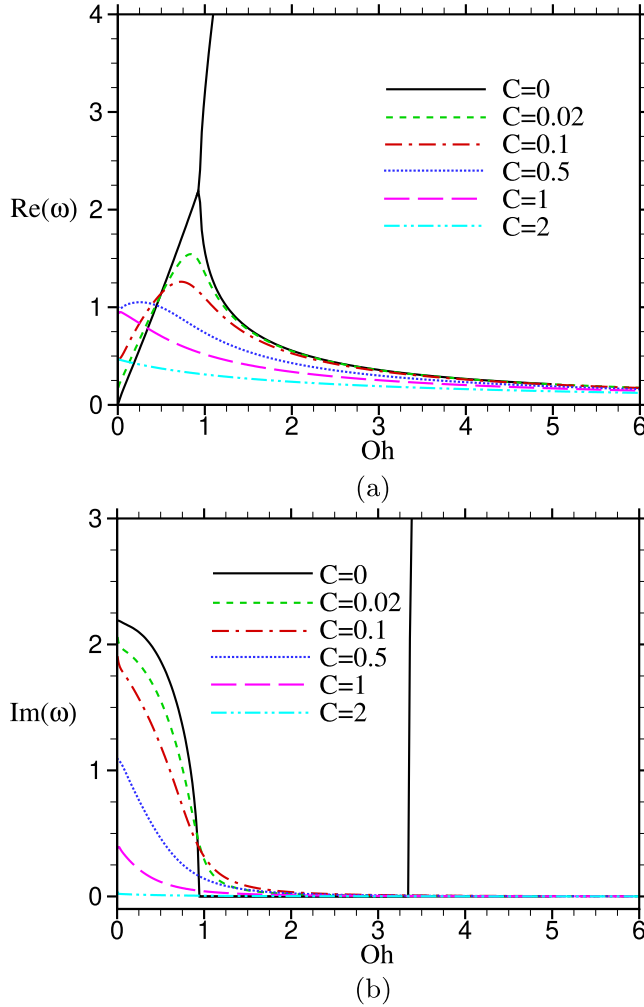


FIG. 7. (a) The damping rate  $Re(\omega)$  and (b) the angular frequency  $Im(\omega)$  versus the Ohnesorge number of the inner liquid  $Oh$  for different values of the Ohnesorge number of the outer liquid  $C$ . The case of relatively small elasticity of the inner liquid,  $\lambda_{1r,i} = 0.018$ ,  $\lambda_{2r,i} = 0.0018$ .  $\rho_r = 1$ .

larger, see the line for  $C = 1$ , the bifurcation phenomenon vanishes. As  $C$  further increases, both the damping rate and the angular frequency are decreased greatly. Particularly, when  $C$  is equal to 2, the angular frequency of the least damped mode is decreased nearly to zero for all values of  $\lambda_{1r,i}$ .

### C. Effect of the elasticity of the outer liquid on the oscillation of the viscoelastic droplet

When the outer host liquid is non-Newtonian viscoelastic, four dimensionless parameters, i.e.,  $\rho_r$ ,  $\eta_{0r}$ ,  $\lambda_{1r,o}$ , and  $\lambda_{2r,o}$ , are needed to describe its properties. Note that in the calculation we use  $C$  instead of  $\eta_{0r}$  to represent the magnitude of the viscosity of the outer liquid, as performed previously. Owing to the presence of the unknown  $\omega$  in both the Bessel and Hankel functions, the transcendental characteristic Eq. (9) becomes extremely difficult to solve. It is hard as well to get a whole picture, for there are so many parameters involved. In the following, we simply fix the density ratio  $\rho_r$  and the Ohnesorge number of the outer liquid  $C$  to 1 and examine the effect of the elasticity of the outer liquid on the oscillation of the droplet by varying the value of  $\lambda_{1r,o}$  or  $\lambda_{2r,o}$ .

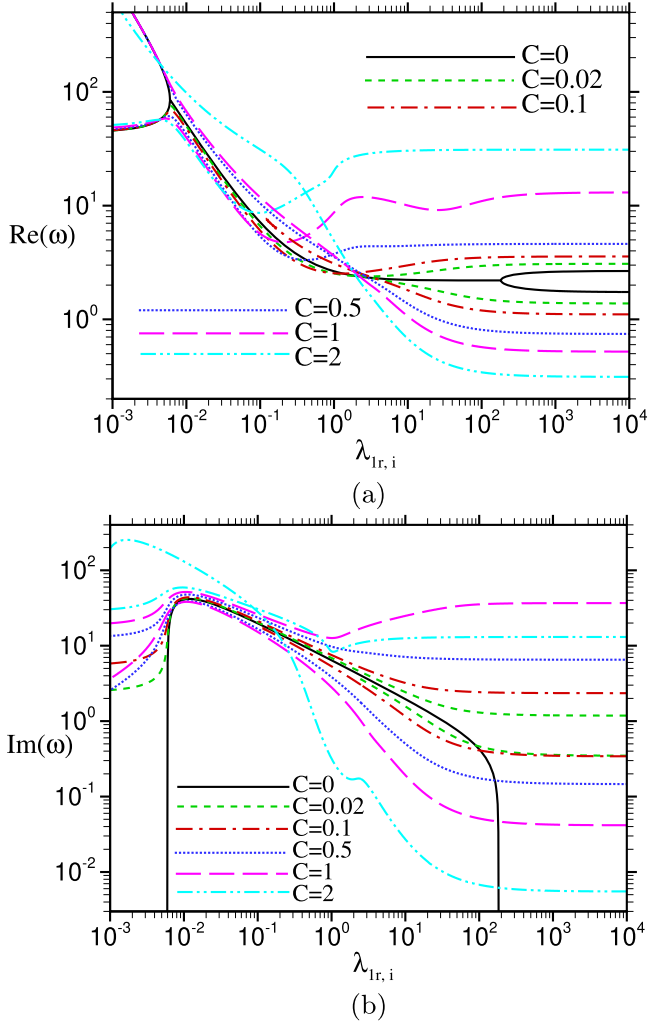


FIG. 8. (a) The damping rate  $\text{Re}(\omega)$  and (b) the angular frequency  $\text{Im}(\omega)$  versus the relative stress relaxation time of the inner liquid  $\lambda_{1r,i}$  for different values of the Ohnesorge number of the outer liquid  $C$ . The case of relatively large viscosity of the inner liquid,  $\text{Oh} = 10$ ,  $\rho_r = 1$ .

The effect of the relative stress relaxation time of the outer liquid  $\lambda_{1r,o}$  on the damping rate and the angular frequency of the viscoelastic droplet is shown in Fig. 10 for the case of large elasticity of the inner liquid. Without loss of generality, in the figure the ratio of  $\lambda_{2r,o}$  to  $\lambda_{1r,o}$  is taken to be 0.1. As can be seen in Fig. 10, with the increase in  $\lambda_{1r,o}$  from zero, both the damping rate and the angular frequency of the least damped mode are suppressed, particularly at small values of  $\text{Oh}$ . When  $\lambda_{1r,o}$  is increased to 1, the angular frequency is decreased almost to zero, indicating that large elasticities of the outer liquid do not favor periodic oscillations of the droplet. For  $\lambda_{1r,o} = 100$ , the line of the second least damped mode is also plotted in the figure. Clearly, for such a large value of  $\lambda_{1r,o}$ , the second least damped mode comes into play with its damping rate comparable to that of the least damped mode and its nonzero angular frequency. Presumably, the elasticity of the outer liquid may lead to a multimode dominant situation in which two or more modes are of nearly equal importance in determining the oscillation characteristics of the droplet.

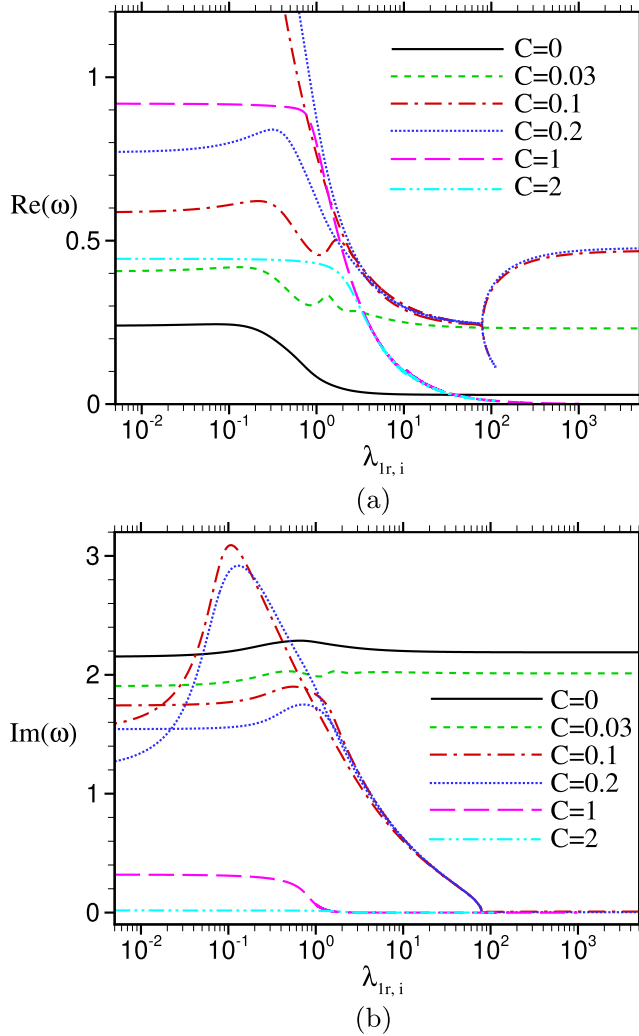


FIG. 9. (a) The damping rate  $\text{Re}(\omega)$  and (b) the angular frequency  $\text{Im}(\omega)$  versus the relative stress relaxation time of the inner liquid  $\lambda_{1r,i}$  for different values of the Ohnesorge number of the outer liquid  $C$ . The case of relatively small viscosity of the inner liquid,  $\text{Oh} = 0.1$ .  $\rho_r = 1$ .

The small elasticity case of the inner liquid is shown in Fig. 11, which turns out to be similar to the large elasticity case in Fig. 10. In the small elasticity case, both the damping rate and the angular frequency decreases with the increase in  $\lambda_{1r,o}$ . When  $\lambda_{1r,o}$  is as large as 2, the angular frequency approaches zero, indicating that the decay of the least damped mode becomes almost aperiodic.

The effect of the relative strain retardation time of the outer host liquid  $\lambda_{2r,o}$  on the oscillation of the viscoelastic droplet is shown in Fig. 12, where the large elasticity case of the inner liquid is considered and the relative stress relaxation time of the outer liquid  $\lambda_{1r,o}$  is fixed to 1. As shown in the figure, as the ratio of  $\lambda_{2r,o}$  to  $\lambda_{1r,o}$  increases, both the damping rate and the angular frequency are increased. However, the effect of  $\lambda_{2r,o}$  is quite limited. We predict that compared with the other properties of the outer liquid the strain retardation time is a secondary factor in the oscillation of the droplet.

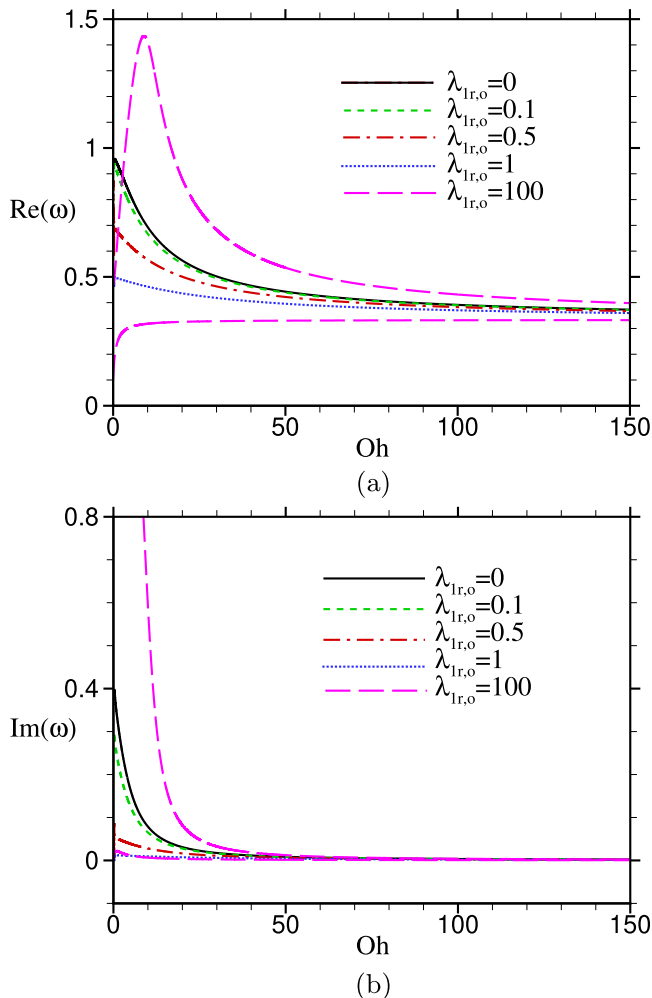


FIG. 10. (a) The damping rate  $\text{Re}(\omega)$  and (b) the angular frequency  $\text{Im}(\omega)$  versus the Ohnesorge number of the inner liquid  $\text{Oh}$  for different values of the relative stress relaxation time of the outer liquid  $\lambda_{1r,o}$ . The case of relatively large elasticity of the inner liquid,  $\lambda_{1r,i} = 30$ ,  $\lambda_{2r,i} = 3$ ,  $\rho_r = 1$ ,  $C = 1$ .

#### IV. CONCLUSIONS

The small-amplitude oscillation of a viscoelastic liquid droplet suspended in an immiscible viscoelastic host liquid is studied. The damping rate and the angular frequency determining the oscillation behavior of the viscoelastic droplet are obtained by solving numerically the characteristic equation derived. The effect of the density, viscosity and elasticity of the outer host liquid on the oscillation of the viscoelastic droplet is explored. It is found that within the interval of Ohnesorge number in which the droplet is periodically oscillatory, increasing the density of the outer liquid leads to a general decrease in the damping rate and in the frequency of oscillation. The region in the parametric plane of  $\text{Oh}$  and  $\lambda_{1r,i}$ , where the droplet undergoes periodic oscillations, can be enlarged to some extent by making the outer liquid denser. The viscosity of the outer liquid may lead to the disappearance of supercritical and subcritical bifurcation phenomena existing in the inviscid case of the outer liquid. When the outer liquid is viscous, the transition from periodic oscillation to aperiodic decay is absent and the droplet oscillates periodically. In addition, the viscosity of

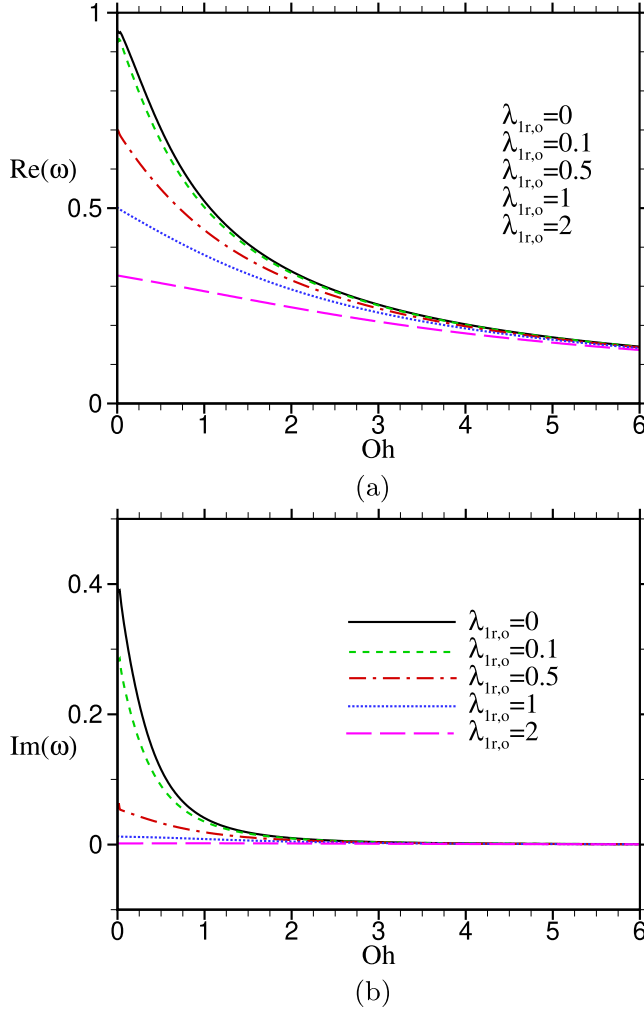


FIG. 11. (a) The damping rate  $Re(\omega)$  and (b) the angular frequency  $Im(\omega)$  versus the Ohnesorge number of the inner liquid  $Oh$  for different values of the relative stress relaxation time of the outer liquid  $\lambda_{1r,o}$ . The case of relatively small elasticity of the inner liquid,  $\lambda_{1r,i} = 0.018$ ,  $\lambda_{2r,i} = 0.0018$ .  $\rho_r = 1$ ,  $C = 1$ .

the inner or outer liquid is found to play a dual role in the oscillation of the droplet. Depending on the magnitude of viscosity, it enhances/retards the damping of a perturbation by dissipating energy/diffusing vorticities. The elasticity of the outer host liquid may result in a decrease in both the damping rate and the angular frequency of the least damped mode.

#### ACKNOWLEDGMENT

This work was supported by the National Natural Science Foundation of China, Projects No. 11772328 and No. 11621202.

#### APPENDIX: DERIVATION OF THE CHARACTERISTIC EQUATION

Substitution of the decomposition Eq. (8) into the Jeffreys Eq. (1) yields

$$\boldsymbol{\tau} = 2\eta_{\text{eff}}\mathbf{D}, \quad (\text{A1})$$

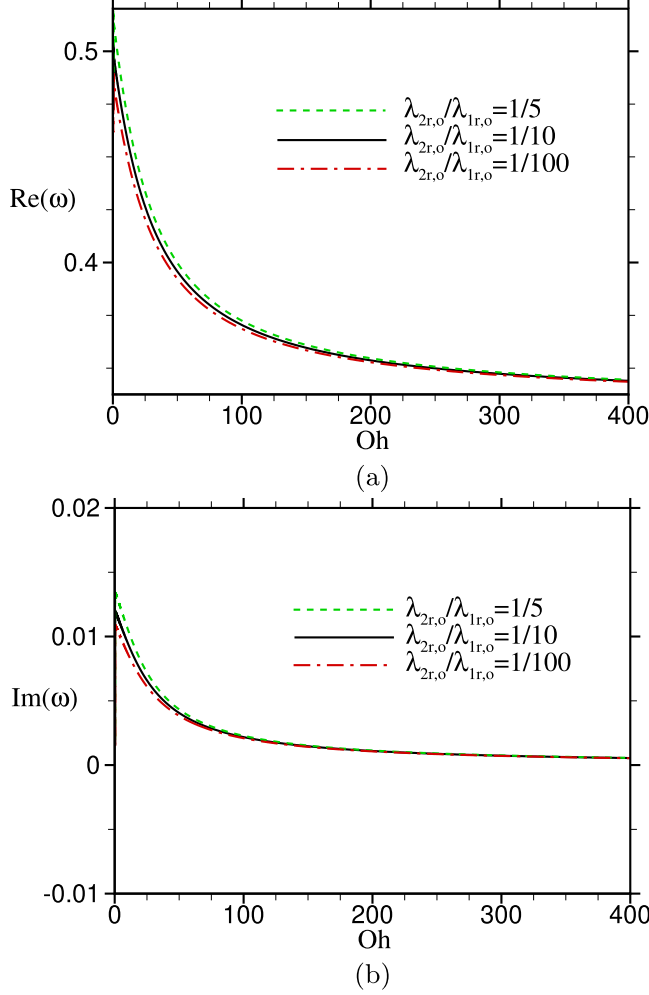


FIG. 12. (a) The damping rate  $Re(\omega)$  and (b) the angular frequency  $Im(\omega)$  versus the Ohnesorge number of the inner liquid  $Oh$  for different values of the relative strain retardation time of the outer liquid  $\lambda_{2r,o}/\lambda_{1r,o}$ . The case of relatively large elasticity of the inner liquid,  $\lambda_{1r,i} = 30$ ,  $\lambda_{2r,i} = 3$ ,  $\rho_r = 1$ ,  $C = 1$ ,  $\lambda_{1r,o} = 1$ .

where  $\eta_{\text{eff}} = \eta_0(1 - \lambda_2\sigma)/(1 - \lambda_1\sigma)$  is the so-called effective viscosity [10,11].

Then the momentum Eq. (3) is expressed as

$$\rho \frac{\partial \mathbf{v}}{\partial t} = -\nabla p + \eta_{\text{eff}} \nabla^2 \mathbf{v}. \quad (\text{A2})$$

Taking the curl of Eq. (A2), we have

$$\rho \frac{\partial \boldsymbol{\Omega}}{\partial t} = -\eta_{\text{eff}} \nabla \times \nabla \times \boldsymbol{\Omega}, \quad (\text{A3})$$

where  $\boldsymbol{\Omega} = \nabla \times \mathbf{v}$  is the vorticity.

As is known, the vorticity field is solenoidal, which can be decomposed into a toroidal and a poloidal field [21,22], i.e.,

$$\boldsymbol{\Omega} = \nabla \times \mathbf{A} + \nabla \times \nabla \times \mathbf{B}, \quad (\text{A4})$$

where the vectors  $\mathbf{A}$  and  $\mathbf{B}$  only have a nonzero component in the radial direction. Thus, the velocity field consists of three components,

$$\mathbf{v} = \mathbf{A} + \nabla \times \mathbf{B} + \nabla \phi, \quad (\text{A5})$$

where  $\phi$  is the velocity potential. The second component,  $\nabla \times \mathbf{B}$ , is a tangential part of the velocity, corresponding to the purely rotational motion of the liquids. Because there is no restoring force for this motion, it will be aperiodically damped ultimately [22,26]. One can also find that the governing equations and boundary conditions in which  $\mathbf{B}$  is involved are decoupled with those equations of  $\mathbf{A}$  and  $\phi$ . As a consequence, the component  $\mathbf{B}$  is of little interest and can be omitted appropriately.

Impose the normal mode decomposition

$$\mathbf{A} = T(r)P_n^m(\cos\theta)e^{im\varphi}e^{-\sigma t}\mathbf{e}_r, \quad (\text{A6})$$

where  $\mathbf{e}_r$  is the unit vector in the radial direction, and substitute it into Eq. (A3), we get an equation for  $T$ ,

$$\frac{d^2T}{dr^2} - \frac{n(n+1)}{r^2}T + \frac{\rho\sigma}{\eta_{\text{eff}}}T = 0. \quad (\text{A7})$$

Considering the boundedness at  $r = 0$  and  $r \rightarrow \infty$ , the solutions to Eq. (A7) are

$$T_i(r) = \left(\frac{r}{R}\right)^{\frac{1}{2}} T_i(R) \frac{J_{n+\frac{1}{2}}(x_i)}{J_{n+\frac{1}{2}}(X_i)}, \quad (\text{A8})$$

$$T_o(r) = \left(\frac{r}{R}\right)^{\frac{1}{2}} T_o(R) \frac{H_{n+\frac{1}{2}}^{(1)}(x_o)}{H_{n+\frac{1}{2}}^{(1)}(X_o)}, \quad (\text{A9})$$

where

$$x = \sqrt{\frac{\rho\sigma}{\eta_{\text{eff}}}}r, \quad X = \sqrt{\frac{\rho\sigma}{\eta_{\text{eff}}}}R. \quad (\text{A10})$$

However, from the continuity Eq. (2), we get an equation for the velocity potential  $\phi$ ,

$$\nabla^2\phi = -\nabla \cdot \mathbf{A} = -\frac{1}{r^2} \frac{d}{dr}(r^2T)P_n^m(\cos\theta)e^{im\varphi}e^{-\sigma t}. \quad (\text{A11})$$

Similarly, substituting the normal mode decomposition

$$\phi = \Phi(r)P_n^m(\cos\theta)e^{im\varphi}e^{-\sigma t} \quad (\text{A12})$$

into Eq. (A11) yields

$$\frac{d^2\Phi}{dr^2} + \frac{2}{r} \frac{d\Phi}{dr} - \frac{n(n+1)}{r^2}\Phi = -\frac{1}{r^2} \frac{d}{dr}(r^2T). \quad (\text{A13})$$

The general solution to Eq. (A13) is

$$\Phi = \left[ \alpha - \frac{n+1}{2n+1} \int_R^r s^{-n}T(s)ds \right] r^n + \left[ \beta - \frac{n}{2n+1} \int_R^r s^{n+1}T(s)ds \right] r^{-(n+1)}, \quad (\text{A14})$$

where  $\alpha$  and  $\beta$  are integration constants. The boundedness at  $r = 0$  and  $r \rightarrow \infty$  requires that

$$\beta_i = -\frac{n}{2n+1} \int_0^R r^{n+1}T(r)dr \quad (\text{A15})$$

and

$$\alpha_o = \frac{n+1}{2n+1} \int_R^\infty r^{-n}T(r)dr. \quad (\text{A16})$$

From the momentum Eq. (A2) we express the pressure as

$$\hat{p}(r) = \rho\sigma\Phi - \eta_{\text{eff}} \frac{dT}{dr}. \quad (\text{A17})$$

Plugging  $T$  in Eqs. (A8) and (A9),  $\Phi$  in Eq. (A14), and  $\hat{p}$  in Eq. (A17) into the boundary condition Eqs. (4)–(7), we have

$$T_i(R) + \frac{d\Phi_i}{dr} \Big|_{r=R} = -\sigma\hat{\xi}, \quad (\text{A18})$$

$$T_o(R) + \frac{d\Phi_o}{dr} \Big|_{r=R} = -\sigma\hat{\xi}, \quad (\text{A19})$$

$$\Phi_i(R) = \Phi_o(R), \quad (\text{A20})$$

$$2R \frac{d}{dr} \left[ \frac{1}{r} (\eta_{\text{eff},o}\Phi_o - \eta_{\text{eff},i}\Phi_i) \right] \Big|_{r=R} + \eta_{\text{eff},o}T_o(R) - \eta_{\text{eff},i}T_i(R) = 0, \quad (\text{A21})$$

$$-\hat{p}_o(R) + 2\eta_{\text{eff},o} \left( \frac{dT_o}{dr} + \frac{d^2\Phi_o}{dr^2} \right) \Big|_{r=R} + \hat{p}_i(R) - 2\eta_{\text{eff},i} \left( \frac{dT_i}{dr} + \frac{d^2\Phi_i}{dr^2} \right) \Big|_{r=R} = \gamma \frac{(n-1)(n+2)}{R^2} \hat{\xi}. \quad (\text{A22})$$

Substituting Eq. (A14) into the kinematic boundary condition Eqs. (A18) and (A19) yields

$$\alpha_i = \frac{n+1}{n} R^{-(2n+1)} \beta_i - \frac{\sigma}{n} R^{-(n-1)} \hat{\xi}, \quad (\text{A23})$$

$$\beta_o = \frac{n}{n+1} R^{2n+1} \alpha_o + \frac{\sigma}{n+1} R^{n+2} \hat{\xi}. \quad (\text{A24})$$

Substituting Eq. (A14) as well as Eqs. (A23) and (A24) into the no-slip boundary condition Eq. (A20) and the continuity of the tangential stresses Eq. (A21) yields

$$nR^{n-1} \alpha_o - (n+1)R^{-(n+2)} \beta_i = -\sigma\hat{\xi}, \quad (\text{A25})$$

and

$$\begin{aligned} & 2n(2n+1)\eta_{\text{eff},o}R^{n-1}\alpha_o - 2(n+1)(2n+1)\eta_{\text{eff},i}R^{-(n+2)}\beta_i + n(n+1)[\eta_{\text{eff},o}T_o(R) - \eta_{\text{eff},i}T_i(R)] \\ & = -2[n(n+2)\eta_{\text{eff},o} - (n-1)(n+1)\eta_{\text{eff},i}]\sigma\hat{\xi}. \end{aligned} \quad (\text{A26})$$

Substitution of the solutions of  $T$ , i.e., Eqs. (A8) and (A9), into Eqs. (A15) and (A16) yields

$$\beta_i = -\frac{n}{2n+1} \frac{T_i(R)R^{n+2}}{X_i J_{n+\frac{1}{2}}(X_i)/J_{n+\frac{3}{2}}(X_i)} \quad (\text{A27})$$

and

$$\alpha_o = \frac{n+1}{2n+1} \frac{T_o(R)R^{-(n-1)}}{X_o H_{n+\frac{1}{2}}^{(1)}(X_o)/H_{n-\frac{1}{2}}^{(1)}(X_o)}. \quad (\text{A28})$$

Now substituting Eqs. (A27) and (A28) into Eqs. (A25) and (A26), we obtain the following expressions of  $T_i(R)$  and  $T_o(R)$ :

$$T_i(R) = \frac{(2n+1)\eta_{\text{eff},o}X_o \frac{H_{n+\frac{1}{2}}^{(1)}(X_o)}{H_{n-\frac{1}{2}}^{(1)}(X_o)} - 2(n-1)(n+1)(\eta_{\text{eff},o} - \eta_{\text{eff},i})}{n(n+1)[2(\eta_{\text{eff},i} - \eta_{\text{eff},o}) - \eta_{\text{eff},i}X_i \frac{J_{n+\frac{1}{2}}(X_i)}{J_{n+\frac{3}{2}}(X_i)} - \eta_{\text{eff},o}X_o \frac{H_{n+\frac{1}{2}}^{(1)}(X_o)}{H_{n-\frac{1}{2}}^{(1)}(X_o)}]} X_i \frac{J_{n+\frac{1}{2}}(X_i)}{J_{n+\frac{3}{2}}(X_i)} \sigma\hat{\xi}, \quad (\text{A29})$$

$$T_o(R) = \frac{(2n+1)\eta_{\text{eff},i} X_i \frac{J_{n+\frac{1}{2}}(X_i)}{J_{n+\frac{3}{2}}(X_i)} + 2n(n+2)(\eta_{\text{eff},o} - \eta_{\text{eff},i})}{n(n+1)\left[2(\eta_{\text{eff},i} - \eta_{\text{eff},o}) - \eta_{\text{eff},i} X_i \frac{J_{n+\frac{1}{2}}(X_i)}{J_{n+\frac{3}{2}}(X_i)} - \eta_{\text{eff},o} X_o \frac{H_{n+\frac{1}{2}}^{(1)}(X_o)}{H_{n-\frac{1}{2}}^{(1)}(X_o)}\right]} X_o \frac{H_{n+\frac{1}{2}}^{(1)}(X_o)}{H_{n-\frac{1}{2}}^{(1)}(X_o)} \sigma \hat{\xi}. \quad (\text{A30})$$

The pressures at the interface can be obtained by substituting Eqs. (A14), (A23), (A24), (A27), and (A28) into Eq. (A17),

$$\hat{p}_i(R) = -(n+1)\eta_{\text{eff},i} \frac{T_i(R)}{R} - \rho_i R \sigma^2 \frac{\hat{\xi}}{n}, \quad (\text{A31})$$

$$\hat{p}_o(R) = n\eta_{\text{eff},o} \frac{T_o(R)}{R} + \rho_o R \sigma^2 \frac{\hat{\xi}}{n+1}. \quad (\text{A32})$$

Then substituting Eqs. (A31) and (A32) into the normal force balance Eq. (A22) yields

$$\left[ \left( \frac{\rho_o}{n+1} + \frac{\rho_i}{n} \right) \sigma^2 R + 2(n-1)(n+2)(\eta_{\text{eff},o} - \eta_{\text{eff},i}) \frac{\sigma}{R} + (n-1)(n+2) \frac{\gamma}{R^2} \right] \hat{\xi} + n(n+2)\eta_{\text{eff},o} \frac{T_o(R)}{R} - (n-1)(n+1)\eta_{\text{eff},i} \frac{T_i(R)}{R} = 0. \quad (\text{A33})$$

Finally substituting Eqs. (A29) and (A30) into Eq. (A33), we obtain the following characteristic equation:

$$\frac{\sigma_0^2}{\sigma^2} = -1 + \frac{\left[ (2n+1)\eta_{\text{eff},i} X_i \frac{J_{n+\frac{1}{2}}(X_i)}{J_{n+\frac{3}{2}}(X_i)} + 2n(n+2)(\eta_{\text{eff},o} - \eta_{\text{eff},i}) \right] \left[ (2n+1)\eta_{\text{eff},o} X_o \frac{H_{n+\frac{1}{2}}^{(1)}(X_o)}{H_{n-\frac{1}{2}}^{(1)}(X_o)} - 2(n-1)(n+1)(\eta_{\text{eff},o} - \eta_{\text{eff},i}) \right]}{\sigma R^2 [n\rho_o + (n+1)\rho_i] \left[ \eta_{\text{eff},i} X_i \frac{J_{n+\frac{1}{2}}(X_i)}{J_{n+\frac{3}{2}}(X_i)} + \eta_{\text{eff},o} X_o \frac{H_{n+\frac{1}{2}}^{(1)}(X_o)}{H_{n-\frac{1}{2}}^{(1)}(X_o)} + 2(\eta_{\text{eff},o} - \eta_{\text{eff},i}) \right]}, \quad (\text{A34})$$

where

$$\sigma_0^2 = \frac{(n-1)n(n+1)(n+2)}{n\rho_o + (n+1)\rho_i} \frac{\gamma}{R^3}. \quad (\text{A35})$$

Recall that  $\sigma_0$  is the frequency of oscillation of the inviscid problem [21,22].

- 
- [1] L. Rayleigh, On the capillary phenomena of jets, *Proc. R. Soc. London A* **29**, 71 (1879).
  - [2] L. Kelvin, *Mathematical and Physical Papers* (Clay and Sons, London, 1890).
  - [3] H. Lamb, On the oscillations of a viscous spheroid, *Proc. Lond. Math. Soc.* **s1-13**, 51 (1881/82).
  - [4] S. Chandrasekhar, The oscillations of a viscous liquid globe, *Proc. Lond. Math. Soc.* **s3-9**, 141 (1959).
  - [5] W. H. Reid, The oscillations of a viscous liquid drop, *Q. Appl. Math.* **18**, 86 (1960).
  - [6] A. Prosperetti, Free oscillations of drops and bubbles: The initial-value problem, *J. Fluid Mech.* **100**, 333 (1980).
  - [7] S. Arcidiacono, D. Poulidakos, and Y. Ventikos, Oscillatory behavior of nanodroplets, *Phys. Rev. E* **70**, 011505 (2004).
  - [8] H. F. Bauer, Surface and interface oscillations in an immiscible spherical visco-elastic system, *Acta Mech.* **56**, 127 (1985).
  - [9] H. F. Bauer and W. Eidel, Vibrations of a visco-elastic spherical immiscible liquid system, *Z. Angew. Math. Mech.* **67**, 525 (1987).
  - [10] D. B. Khismatullin and A. Nadim, Shape oscillations of a viscoelastic drop, *Phys. Rev. E* **63**, 061508 (2001).
  - [11] G. Brenn and S. Teichtmeister, Linear shape oscillations and polymeric time scales of viscoelastic drops, *J. Fluid Mech.* **733**, 504 (2013).

- [12] G. Brenn and G. Plohl, The oscillating drop method for measuring the deformation retardation time of viscoelastic liquids, *J. Non-Newtonian Fluid Mech.* **223**, 88 (2015).
- [13] S. D. Hoath, W. K. Hsiao, G. D. Martin, S. Jung, S. A. Butler, N. F. Morrison, O. G. Harlen, L. S. Yang, C. D. Bain, and I. M. Hutchings, Oscillations of aqueous PEDOT:PSS fluid droplets and the properties of complex fluids in drop-on-demand inkjet printing, *J. Non-Newtonian Fluid Mech.* **223**, 28 (2015).
- [14] E. Becker, W. J. Hiller, and T. A. Kowalewski, Experimental and theoretical investigation of large-amplitude oscillations of liquid droplets, *J. Fluid Mech.* **231**, 189 (1991).
- [15] H. Azuma and S. Yoshihara, Three-dimensional large-amplitude drop oscillations: Experiments and theoretical analysis, *J. Fluid Mech.* **393**, 309 (1999).
- [16] E. H. Trinh, D. B. Thiessen, and R. G. Holt, Driven and freely decaying nonlinear shape oscillations of drops and bubbles immersed in a liquid: Experimental results, *J. Fluid Mech.* **364**, 253 (1998).
- [17] O. A. Basaran, Nonlinear oscillations of viscous liquid drops, *J. Fluid Mech.* **241**, 169 (1992).
- [18] T. Shi and R. E. Apfel, Oscillations of a deformed liquid drop in an acoustic field, *Phys. Fluids* **7**, 1545 (1995).
- [19] B. M. Rush and A. Nadim, The shape oscillations of a two-dimensional drop including viscous effects, *Eng. Anal. Bound. Elem.* **24**, 43 (2000).
- [20] W. R. Smith, Modulation equations for strongly nonlinear oscillations of an incompressible viscous drop, *J. Fluid Mech.* **654**, 141 (2010).
- [21] C. A. Miller and L. E. Scriven, The oscillations of a fluid droplet immersed in another fluid, *J. Fluid Mech.* **32**, 417 (1968).
- [22] A. Prosperetti, Normal-mode analysis for the oscillations of a viscous liquid drop in an immiscible liquid, *J. Méc.* **19**, 149 (1980).
- [23] P. L. Marston, Shape oscillation and static deformation of drops and bubbles driven by modulated radiation stresses-theory, *J. Acoust. Soc. Am.* **67**, 15 (1980).
- [24] O. A. Basaran, T. C. Scott, and C. H. Byers, Drop oscillations in liquid-liquid systems, *AIChE J.* **35**, 1263 (1989).
- [25] Y. Bayazitogh and P. V. R. Suryanarayana, Dynamics of oscillating viscous droplets immersed in viscous media, *Acta Mech.* **95**, 167 (1992).
- [26] D. L. Whitaker, C. Kim, C. L. Vicente, M. A. Weilert, H. J. Maris, and G. M. Seidel, Theory of the small amplitude shape oscillations of a helium-ii drop, *J. Low Temp. Phys.* **114**, 523 (1999).
- [27] J. C. Crispell, R. Cortez, D. B. Khismatullin, and L. J. Fauci, Shape oscillations of a droplet in an Oldroyd-B fluid, *Phys. D* **240**, 1593 (2011).
- [28] K. Sarkar and W. R. Schowalter, Deformation of a viscoelastic drop in time-periodic extensional flows at non-zero Reynolds number, *J. Non-Newtonian Fluid Mech.* **95**, 315 (2000).
- [29] K. Sarkar and W. R. Schowalter, Deformation of a two-dimensional drop at non-zero Reynolds number in time-periodic extensional flows: Numerical simulation, *J. Fluid Mech.* **436**, 177 (2001).
- [30] K. Sarkar and W. R. Schowalter, Deformation of a two-dimensional drop at non-zero Reynolds number in time-periodic extensional flows: Analytic treatment, *J. Fluid Mech.* **436**, 207 (2001).
- [31] X. Li and K. Sarkar, Drop dynamics in an oscillating extensional flow at finite Reynolds numbers, *Phys. Fluids* **17**, 027103 (2005).
- [32] X. Li and K. Sarkar, Drop deformation and breakup in a potential vortex, *J. Fluid Mech.* **564**, 1 (2006).
- [33] N. Aggarwal and K. Sarkar, Effects of matrix viscoelasticity on viscous and viscoelastic drop deformation in a shear flow, *J. Fluid Mech.* **601**, 63 (2008).
- [34] IMSL, *MATH/LIBRARY: FORTRAN Subroutines for Mathematical Applications: User's Manual* (IMSL, Houston, TX, 1987).
- [35] F. Li, X. Y. Yin, and X. Z. Yin, Small-amplitude shape oscillation and linear instability of an electrically charged viscoelastic liquid droplet, *J. Non-Newtonian Fluid Mech.* **264**, 85 (2019).